

## Mesonic correlations and quark deconfinement

D. Blaschke

*Fachbereich Physik, Universität Rostock, D-18051 Rostock, Germany*  
*E-mail: blaschke@darss.mpg.uni-rostock.de*

P.C. Tandy

*Center for Nuclear Research, Department of Physics, Kent State University*  
*Kent, OH 44242, USA*  
*E-mail: tandy@cnr2.kent.edu*

A simple confining separable interaction Ansatz for the rainbow-ladder truncated QCD Dyson-Schwinger equations is used to implement chiral restoration and quark deconfinement in a study of  $q\bar{q}$  meson states at finite temperature. The model is fixed at  $T = 0$  by reproducing selected  $\pi$  and  $\rho$  properties. Deconfinement and chiral restoration are found to both occur at  $T_c = 146$  MeV. In the pion sector, we investigate  $M_\pi(T)$  and  $f_\pi(T)$  along with the exact QCD mass relation and the GMOR relation. For the vector mode, we investigate the 3-space transverse and longitudinal masses  $M_\rho^T(T)$  and  $M_\rho^L(T)$ , along with the width for the decay  $\rho^0 \rightarrow e^+e^-$ . The equation of state (EOS) for the model is investigated in the  $T - \mu$  plane, a tri-critical point is identified and the relationship to a bag model is discussed. The deconfinement transition in rapidly rotating neutron stars is considered and a new signal from the pulsar timing in binary systems with mass accretion is suggested. The model is used to discuss the possibility of a superconducting quark matter phase.

### 1 Introduction

The experimental search for the QCD deconfinement phase transition in ultrarelativistic heavy-ion collisions will enter a new stage when the relativistic heavy-ion collider (RHIC) at Brookhaven will provide data complementary to those from the CERN SPS<sup>1</sup>. It is desirable to have a continuum field-theoretical modeling of quark deconfinement and chiral restoration at finite temperature and density (or chemical potential  $\mu$ ) that can be extended also to hadronic observables in a rapid and transparent way. Significant steps in this direction have recently been taken through a continuum approach to  $\text{QCD}_{T,\mu}$  based on the truncated Dyson-Schwinger equations (DSEs) within the Matsubara formalism<sup>2,3,4</sup> and a recent review<sup>5</sup> is available. A most appealing feature of this approach to modeling nonperturbative  $\text{QCD}_{T,\mu}$  is that dynamical chiral symmetry breaking *and* confinement is embodied in the the model gluon 2-point function constrained by chiral observables at  $T = \mu = 0$  and no new parameters are needed for extension to  $T, \mu > 0$ . Approximations introduced by a specific truncation scheme for the set of DSEs can be systematically

relaxed. However due to the breaking of  $O(4)$  symmetry and the number of discrete Matsubara modes needed, the finite  $T, \mu$  extension of realistic DSE models entails solution of a complicated set of coupled integral equations. The generation of hadronic observables from such solutions, although a straightforward adaption of the approach<sup>6</sup> found to be successful at  $T = \mu = 0$ , adds further to the difficulties. In the separable model we study here, detailed realism is sacrificed in the hope that the dominant and essential features may be captured in a simple and transparent format. To this end we simplify an existing  $T = \mu = 0$  confining separable interaction Ansatz<sup>7</sup> to produce a gaussian separable model for  $T, \mu > 0$ <sup>8</sup>.

## 2 Confining separable Dyson-Schwinger equation model

In a Feynman-like gauge where we take  $D_{\mu\nu} = \delta_{\mu\nu}D(p - q)$  to be the effective interaction between quark colored vector currents, the rainbow approximation to the DSE for the quark propagator  $S(p) = [i\not{p}A(p) + B(p) + m_0]^{-1}$  yields in Euclidean metric

$$B(p) = \frac{16}{3} \int \frac{d^4q}{(2\pi)^4} D(p - q) \frac{B(q) + m_0}{q^2 A^2(q) + [B(q) + m_0]^2} , \quad (1)$$

$$[A(p) - 1]p^2 = \frac{8}{3} \int \frac{d^4q}{(2\pi)^4} D(p - q) \frac{(p \cdot q)A(q)}{q^2 A^2(q) + [B(q) + m_0]^2} . \quad (2)$$

We study a separable interaction given by<sup>7</sup>

$$D(p - q) = D_0 f_0(p^2)f_0(q^2) + D_1 f_1(p^2)(p \cdot q)f_1(q^2) , \quad (3)$$

where  $D_0, D_1$  are strength parameters and the form factors, for simplicity, are here taken to be  $f_i(p^2) = \exp(-p^2/\Lambda_i^2)$  with range parameters  $\Lambda_i$ . It is easily verified that if  $D_0$  is non-zero, then  $B(p) = \Delta m f_0(p^2)$ , and if  $D_1$  is non-zero, then  $A(p) = 1 + \Delta a f_1(p^2)$ . The DSE then reduces to nonlinear equations for the constants  $\Delta m$  and  $\Delta a$ . The form factors should be chosen to simulate the  $p^2$  dependence of  $A(p)$  and  $B(p)$  from a more realistic interaction. We restrict our considerations here to the rank-1 case where  $D_1 = 0$  and  $A(p) = 1$ . The parameters  $D_0, \Lambda_0$  and  $m_0$  are used to produce reasonable  $\pi$  and  $\omega$  properties as well as to ensure the produced  $B(p)$  has a reasonable strength with a range  $\Lambda_0 \sim 0.6 \dots 0.8$  GeV to be realistic<sup>7</sup>.

If there are no solutions to  $p^2 A^2(p) + (B(p) + m_0)^2 = 0$  for real  $p^2$  then the quarks are confined. If in the chiral limit ( $m_0 = 0$ ) there is a nontrivial solution for  $B(p)$ , then chiral symmetry is dynamical broken. Both phenomena can be implemented in this separable model. In the chiral limit, the model is

confining if  $D_0$  is strong enough to make  $\Delta m/\Lambda_0 \geq 1/\sqrt{2e}$ . Thus for a typical range  $\Lambda_0$ , confinement will typically occur with  $M(p \approx 0) \geq 300$  MeV.

Mesons as  $q\bar{q}$  bound states are described by the Bethe-Salpeter equation which in the ladder approximation for the present approach is

$$-\lambda(P^2)\Gamma(p, P) = \frac{4}{3} \int \frac{d^4q}{(2\pi)^4} D(p-q)\gamma_\mu S(q_+) \Gamma(q, P) S(q_-)\gamma_\mu, \quad (4)$$

where  $q_\pm = q \pm P/2$  and  $P$  is the meson momentum. The meson mass is identified from  $\lambda(P^2 = -M^2) = 1$ . With the rank-1 separable interaction, only the  $\gamma_5$  and the  $\gamma_5 \not{P}$  covariants contribute to the  $\pi^7$ , and here we retain only the dominant term  $\Gamma_\pi(p, P) = i\gamma_5 E_\pi(p, P)$ . For the vector meson, the only surviving form is  $\Gamma_{\rho\mu}(p, P) = \gamma_\mu^T(P) E_\rho(p, P)$ , with  $\gamma_\mu^T(P)$  being the projection of  $\gamma_\mu$  transverse to  $P$ . The separable solutions have the form  $E_i(p, P) = f_0(p^2) C_i(P^2)$ ,  $i = \pi, \rho$ , where the  $C_i$  factor out from Eq. (4).

In the limit where a zero momentum range for the interaction is simulated by  $f_0^2(q^2) \propto \delta^4(q)$ , then the expressions for the various BSE eigenvalues  $\lambda(P^2)$  reduce to those of the Munczek and Nemirovsky<sup>9</sup> model which implements extreme infrared dominance via  $D(p-q) \propto \delta^{(4)}(p-q)$ . The correspondence is not complete because the quark DSE solution in this model has  $A(p) \neq 1$ . The  $T, \mu > 0$  generalization of this infrared dominant (ID) model have been studied recently<sup>3,4</sup>.

### 3 Pion and rho-meson properties

With parameters  $m_0/\Lambda_0 = 0.0096$ ,  $D_0\Lambda_0^2 = 128$  and  $\Lambda_0 = 0.687$  GeV, the present Gaussian separable (GSM) model yields  $M_\pi = 0.14$  GeV,  $M_\rho = M_\omega = 0.783$  GeV,  $f_\pi = 0.104$  GeV, a chiral quark condensate  $\langle \bar{q}q \rangle^{1/3} = -0.248$  GeV, and a  $\rho - \gamma$  coupling constant  $g_\rho = 5.04$ .

The generalization to  $T \neq 0$  is systematically accomplished by transcription of the Euclidean quark 4-momentum via  $q \rightarrow q_n = (\omega_n, \vec{q})$ , where  $\omega_n = (2n+1)\pi T$  are the discrete Matsubara frequencies. The obtained  $T$ -dependence of the mass gap  $\Delta m(T)$  allows for a study of the deconfinement and chiral restoration features of this model. We find that both occur at  $T_c = 146$  MeV where, in the chiral limit, both  $\Delta m(T)$  and  $\langle \bar{q}q \rangle^0$  vanish sharply as  $(1 - T/T_c)^\beta$  with the critical exponent having the mean field value  $\beta = 1/2$ .

For the  $\bar{q}q$  meson modes, the  $O(4)$  symmetry is broken and the type of mass shell condition employed must be specified. If there is a bound state, the associated pole contribution to the relevant  $\bar{q}q$  propagator or current correlator will have a denominator proportional to

$$1 - \lambda(\Omega_m^2, \vec{P}^2) \propto \Omega_m^2 + \vec{P}^2 + M^2(T). \quad (5)$$

We investigate the meson mode eigenvalues  $\lambda$  using only the lowest meson Matsubara mode ( $\Omega_m = 0$ ) and the continuation  $\vec{P}^2 \rightarrow -M^2$ . The masses so identified are spatial screening masses corresponding to a behavior  $\exp(-Mx)$  in the conjugate 3-space coordinate  $x$  and should correspond to the lowest bound state if one exists.

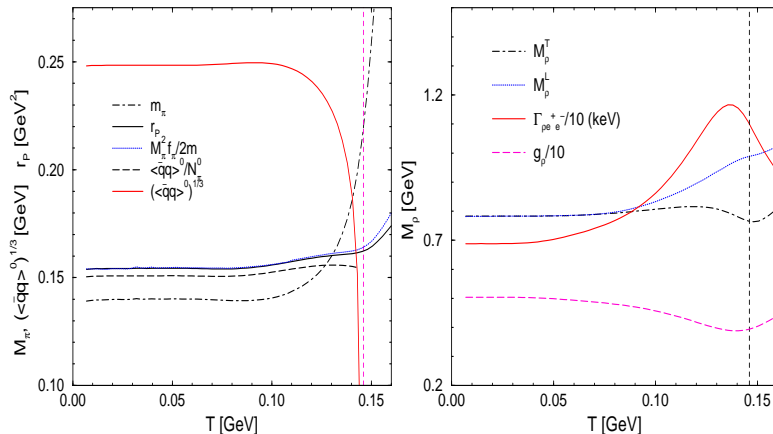


Figure 1:  $T$ -dependence of  $\bar{q}q$  meson properties for the rank-1 separable model up to  $T_c = 146$  MeV. Left panel: Spatial  $M_\pi(T)$  and quantities associated with mass relations as dictated by chiral symmetry; Right panel: Spatial masses  $M_\rho^T(T)$  and  $M_\rho^L(T)$  along with the  $\rho^0 \rightarrow e^+e^-$  decay width and the associated vector coupling constant  $g_\rho(T)$ .

The obtained  $\pi$  and  $\rho$  masses displayed in Fig. 1 and are seen to be only weakly  $T$ -dependent until near  $T_c = 146$  MeV. This result for  $M_\pi(T)$  reproduces the similar behavior obtained from the ladder-rainbow truncation of the DSE-BSE complex with a more realistic interaction<sup>2</sup>. The qualitative behavior obtained for the 3-space transverse and longitudinal masses  $M_\rho^T(T)$ ,  $M_\rho^L(T)$  agrees with that reported<sup>4</sup> for the limiting case of the zero momentum range or ID model.

To explore the extent to which the model respects the detailed constraints from chiral symmetry, we investigate the exact QCD pseudoscalar mass relation<sup>10</sup> which, after extension to  $T > 0$ , is

$$M_\pi^2(T) f_\pi(T) = 2m_0 r_P(T). \quad (6)$$

Here  $r_P$  is the residue at the pion pole in the pseudoscalar vertex, and in the

present model, is given by

$$ir_P(T) = N_c T \sum_n \text{tr}_s \int \frac{d^3q}{(2\pi)^3} \gamma_5 S(q_n + \frac{\vec{P}}{2}) \Gamma_\pi(q_n; \vec{P}) S(q_n - \frac{\vec{P}}{2}). \quad (7)$$

The relation in Eq. (6) is a consequence of the pion pole structure of the isovector axial Ward identity which links the quark propagator, the pseudoscalar vertex and the axial vector vertex<sup>10</sup>. In the chiral limit,  $r_P \rightarrow \langle \bar{q}q \rangle^0 / f_\pi^0$  and Eq.(6), for small mass, produces the Gell-Mann–Oakes–Renner (GMOR) relation.

The exact mass relation, Eq. (6), can only be approximately satisfied when the various quantities are obtained approximately such as in the present separable model. The error can be used to assess the reliability of the present approach to modeling the behavior of the pseudoscalar bound state as the temperature is raised towards  $T_c$ . Our findings are displayed in Fig. 1. There the solid line represents  $r_P(T)$  calculated from the quark loop integral in Eq. (7); the dotted line represents  $r_P$  extracted from the other quantities in Eq. (6). It is surprising that the separable model obeys this exact QCD mass relation to better than 1% for the complete temperature range up to the restoration of chiral symmetry. Also evident from Fig. 1 is that  $M_\pi(T)$  and the chiral condensate are largely temperature independent until within about  $0.8 T_c$  whereafter  $M_\pi$  rises roughly as fast as the condensate falls.

We have also investigated the (approximate) GMOR relation for the present model. The quantity  $\langle \bar{q}q \rangle^0 / N_\pi^0$  is displayed in Fig. 1 as the long-dashed line, and if the GMOR relation were exactly obeyed, this would coincide with  $M_\pi^2 f_\pi / 2m$  which is the dotted line. The quantity  $N_\pi^0$  enters here via its role as the normalization constant of the chiral limit  $\pi$  BS amplitude  $E_\pi^0(p^2) = i\gamma_5 B_0(p^2) / N_\pi^0$ . If all covariants for the pion were to be retained and the axial vector Ward identity were obeyed, one would have  $N_\pi = f_\pi$ <sup>10</sup>. The results in Fig. 1 indicate that the GMOR relation contains an error of about 5% when compared either to the exact mass relation or to the quantities produced by the separable model and that this is temperature-independent until about  $0.9 T_c$ . It should be noted that  $f_\pi^0$ ,  $N_\pi^0$  and  $\langle \bar{q}q \rangle^0$  are equivalent order parameters near  $T_c$  and have weak  $T$ -dependence below  $T_c$ . A consequence is that  $M_\pi^2 f_\pi$ ,  $r_P$  and  $\langle \bar{q}q \rangle^0 / N_\pi^0$  are almost  $T$ -independent and so are the estimated errors for the two mass relations linking these quantities. Since we obtain  $M_\pi$  and  $f_\pi$  from the model BSE solutions at finite current quark mass,  $f_\pi$  does not exactly decrease to zero and  $M_\pi$  does not exactly diverge at  $T_c$ .

Vector mesons play an important role as precursors to di-lepton events in relativistic heavy-ion collisions and it is important to explore the intrinsic  $T$ -dependence of electromagnetic and leptonic vector coupling constants that

can arise from the quark-gluon dynamics that underlies the finite extent of the vector  $\bar{q}q$  modes. The present model provides a simple framework for such investigations. The electromagnetic decay constant  $g_\rho(T)$  that describes the coupling of the transverse  $\rho^0$  to the photon is given by<sup>11</sup>

$$\frac{M_\rho^{T^2}(T)}{g_\rho(T)} = \frac{N_c}{3} T \sum_n \text{tr}_s \int \frac{d^3q}{(2\pi)^3} \gamma_\mu S(q_n + \frac{\vec{P}}{2}) \Gamma_\mu^T(q_n; \vec{P}) S(q_n - \frac{\vec{P}}{2}), \quad (8)$$

after accounting for the normalization<sup>6</sup> of the present BS amplitudes. The electromagnetic decay width of the transverse  $\rho$  mode is calculated from

$$\Gamma_{\rho^0 \rightarrow e^+ e^-}(T) = \frac{4\pi \alpha^2 M_\rho^T(T)}{3 g_\rho^2(T)}. \quad (9)$$

At  $T = 0$  the experimental value is  $\Gamma_{\rho^0 \rightarrow e^+ e^-}(0) = 6.77$  keV corresponding to the value  $g_\rho(0) = 5.03$ . Our results for  $g_\rho(T)$  and  $\Gamma_{\rho^0 \rightarrow e^+ e^-}(T)$  are displayed in Fig. 1. This electromagnetic width of the 3-space transverse  $\rho$  increases with  $T$  and reaches a maximum of 1.72 times the  $T = 0$  width at about  $0.9 T_c$ . An increasing electromagnetic width for the  $\rho$  has been found empirically to be one of the possible medium effects that influence the heavy-ion dilepton spectrum<sup>12</sup>.

#### 4 Equation of state (EOS) for quark matter

The thermodynamical properties of the confining quark model and in particular the EOS and the phase diagram can be obtained from the grand canonical thermodynamical potential  $\Omega(T, V, \mu) = T \ln Z(T, V, \mu) = -p(T, \mu)V$ , where the contributions to the pressure (for a homogeneous system)

$$p(T, \mu) = p_{\text{cond}}(T, \mu) + p_{\text{kin}}(T, \mu) + p_0 \quad (10)$$

are obtained from a mean-field approximation to the Euclidean path integral representation of the grand canonical partition function  $Z(T, V, \mu)$ . In the rank-one separable gluon propagator model, the condensate contribution is  $p_{\text{cond}}(T, \mu) = 3 \Delta m(T, \mu)^2 / (16 D_0)$  and the kinetic part of the quark pressure is given by

$$p_{\text{kin}}(T, \mu) = 2N_c N_f \int \frac{d^3k}{(2\pi)^3} T \sum_n \ln \left( \frac{k_n^2 + M^2(k_n^2)}{k_n^2 + m_0^2} \right) + p_{\text{free}}(T, \mu). \quad (11)$$

In Eq. (11),  $k_n^2 = [(2n+1)\pi T + i\mu]^2 + \mathbf{k}^2$ ,  $M(k_n^2) = m_0 + \Delta m(T, \mu) f_0(k_n^2)$  and the divergent 3-momentum integration has been regularized by subtracting the free quark pressure and adding it in the well-known<sup>13</sup> regularized form

$p_{\text{free}}(T, \mu)$ . The pressure contribution  $p_0$  is found such that the total pressure (10) at the phase boundary in the  $T, \mu$ -plane vanishes, see Fig. 3. While investigating this EOS for the separable confining quark model defined above we have observed that, as a function of the coupling parameter  $D_0$ , an instability  $d(p_{\text{cond}} + p_{\text{kin}})/dT < 0$  occurs when the criterion for confinement (absence of quasiparticle mass poles) is fulfilled. The physical quark pressure in the confinement domain of the phase diagram vanishes, see Fig. 2. The results for the EOS and the phase diagram can be compared to those for the zero momentum range model<sup>3</sup> with the important modification that in the present finite range model the tricritical point is obtained at finite chemical potential whereas with zero range it was found on the  $\mu = 0$  axis of the phase diagram, see Fig. 3. The location of the tricritical point could be experimentally verified in CERN-SPS experiments provided that changes in the pion momentum correlation function could be detected as a function of the beam energy<sup>14</sup>. A

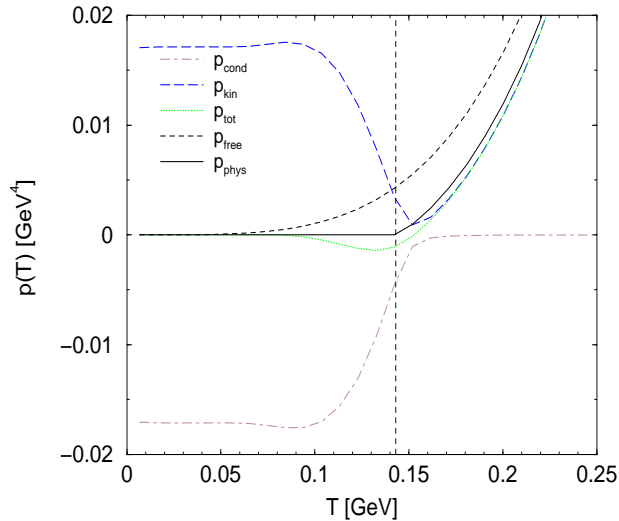


Figure 2: The quark matter pressure as a function of temperature for the separable confining model. The kinetic part (long dashed line) is overcompensated by the condensate part (dot-dashed line) resulting in an instability  $d(p_{\text{cond}} + p_{\text{kin}})/dT < 0$  (dotted line) for  $T < T_c = 146$  MeV which is characteristic for confining quark models. The physical pressure of quark matter (solid line) vanishes in this region. For comparison, the free quark matter pressure is shown by the dashed line.

particularly interesting phenomenological application is the  $T = 0$  quark matter EOS which is a necessary element for studies of quark deconfinement in

neutron stars. The present Gaussian separable model leads<sup>15</sup> to a bag model EOS for quark matter with a bag constant  $B(T = 0) = 150 \text{ MeV}/\text{fm}^3$  for the parameter set ( $D_0 \Lambda_0^2 = 128$ ) employed in Sec. 3. A second parameter set ( $D_0 \Lambda_0^2 = 97$ ) that is also confining and provides an equally good description of the same  $\pi$  and  $\rho$  properties produces  $B(T = 0) = 75 \text{ MeV}/\text{fm}^3$ ; see also Fig. 3. More stringent constraints on the low-temperature EOS will require the inclusion of hadronic excitations including the nucleon.

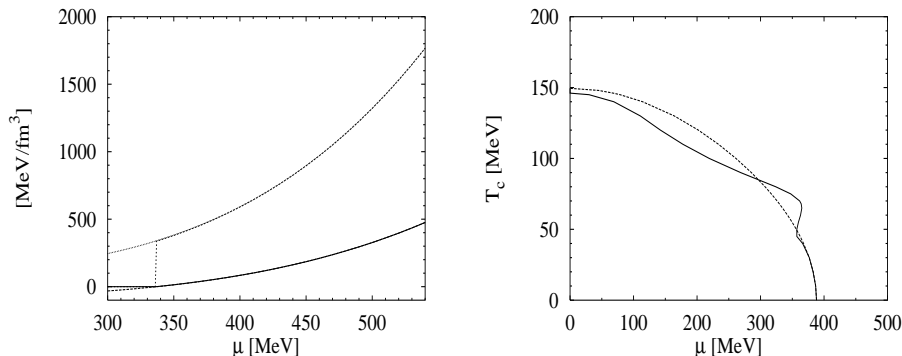


Figure 3: Left panel: pressure (solid line) and energy density (long dashed line) vs. chemical potential at  $T = 0$  for the GSM with  $\Lambda_0 = 0.756 \text{ GeV}$  and  $D_0 \Lambda_0^2 = 97.0$  in the chiral limit. The phase transition from the confining quark matter phase to the deconfined one with restored chiral symmetry occurs at  $\mu = 0.337 \text{ GeV}$  and is first order. The results are coincident with a bag model EOS (dashed and dotted lines) for a bag constant  $B = 75 \text{ MeV}/\text{fm}^3$ . Right panel: quark matter phase diagram for the GSM with  $\Lambda_0 = 0.687 \text{ GeV}$  and  $D_0 \Lambda_0^2 = 128$ . Along the dashed line the pressure vanishes, the solid line separates the chiral symmetric phase from the broken one. A tricritical point is obtained at  $T \sim 127 \text{ MeV}$ ,  $\mu \sim 120 \text{ MeV}$ .

## 5 Deconfinement in rotating neutron stars

For the discussion of deconfinement in neutron stars, it is crucial to go beyond the mean field description and to include into the EOS also the hadronic bound states (neutrons, protons, mesons) in the confined phase. This task has not yet been solved and therefore, we adopt for this phase a Walecka model as it is introduced in<sup>13</sup>. In constructing the phase transition to the deconfined quark matter as described by the GSM with a parameter set leading to  $B = 75 \text{ MeV}/\text{fm}^3$  we have to obey the constraints of global baryon number conservation and charge neutrality<sup>16</sup>. The composition of the neutron star matter is also constrained by the processes which establish  $\beta$ -equilibrium in the quark

phase ( $d \rightarrow u + e^- + \bar{\nu}$ ) and in the hadronic phase ( $n \rightarrow p + e^- + \bar{\nu}$ ). For the given EOS we obtain a deconfinement transition of first order where the hadronic phase is separated from the quark matter one by a mixed phase in the density interval  $1.39 \leq n/n_0 \leq 2.37$ , where  $n_0 = 0.16 \text{ fm}^{-3}$  is the nuclear saturation density<sup>17</sup>.

All observable consequences should be discussed for fastly rotating compact objects and therefore we have studied these rotating configurations using this model-EOS with a deconfinement transition. The result is shown in Fig. 4 and shows that within the present approach a deconfinement transition in compact stars is compatible with constraints on radius and mass recently derived from the observation of QPO in low mass X-ray binaries (LMXBs)<sup>18</sup>. The basic quantity for the study of a deconfinement transition rotating com-

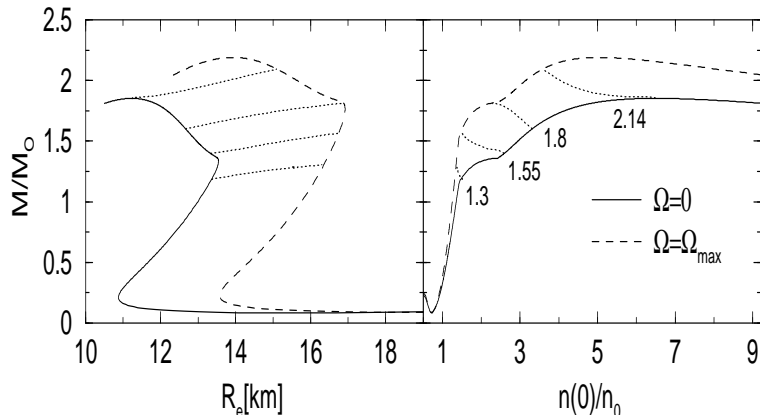


Figure 4: The mass  $M$  as a function of the equatorial radius  $R_e$  (left panel) and the central density (right panel) for a neutron star with deconfinement transition. Rotating configurations (dashed lines) with maximum rotation frequency are connected with the static ones (solid lines) by lines of constant baryon number  $N/N_\odot = 1.3, 1.55, 1.8, 2.14$ , respectively. The occurrence of an extended quark matter core in the compact star is compatible with recently derived constraints on maximum mass and radius from QPO observations in low-mass X-ray binaries, see text.

compact stars is the moment of inertia which governs the rotation and thus the spin-down characteristics. Changes in the angular velocity  $\Omega(t)$  as a function of time can occur, e.g., due to magnetic dipole radiation<sup>19</sup> or mass accretion<sup>17</sup>. During the time evolution of an isolated pulsar, the deviation of the braking index from  $n(\Omega) = 3$  can signal not only the occurrence of a quark matter core, but also its size<sup>17</sup>. We have found that in LMXBs with mass

accretion at conserved angular momentum the occurrence of a quark matter core would reflect itself in a change from a spin-down to spin-up era<sup>17</sup>, see Fig. 5. More detailed investigations of these scenarios have to be performed with a

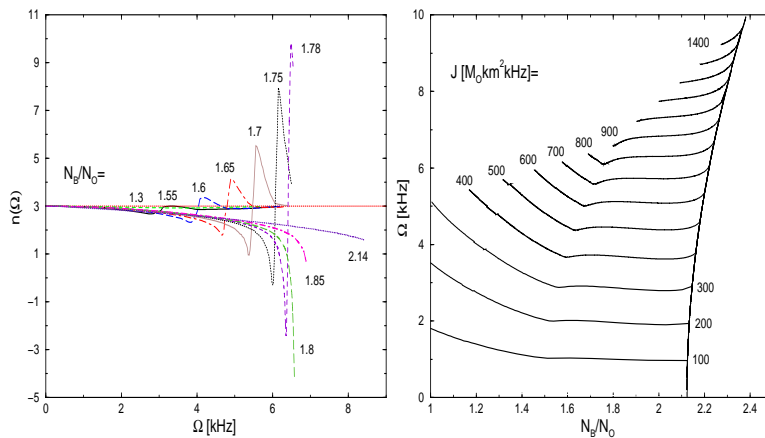


Figure 5: Deconfinement signals from the pulse timing of rapidly rotating compact stars. Left panel: The braking index deviates from  $n = 3$  when during the spin-down evolution of a pulsar a quark matter core is formed which entails a change in the moment of inertia. The larger the radius of the quark core, the more pronounced the signal. Right panel: The spin-down evolution of a compact star with mass accretion at constant angular momentum  $J$  flips to a spin-up behaviour at the onset of deconfinement.

more realistic EOS, in particular for the hadronic phase. The possibility of a  $T = 0$  quark matter EOS which corresponds to a bag model EOS with small bag constants of the order of  $B = 70 \text{ MeV}/\text{fm}^3$  is an important result of the study of the confining quark model which bears interesting consequences for the study of further nontrivial phases in high-density QCD, as e.g. (color-) superconductivity.

## 6 Superconducting quark matter

The possible occurrence of a superconducting quark matter phase<sup>20</sup> has been recently reconsidered on the basis of nonperturbative approaches to the effective quark 4-point interaction<sup>5,21,22,23</sup> and critical temperatures of the order of 50 MeV with diquark pairing gaps of  $\approx 100 \text{ MeV}$  have been obtained. So, if quark matter occurs in the interior of compact stars as advocated in the previous section, then it had to be realised in such a superconducting phase. Deconfinement in compact stars can thus result in effects on the magnetic field

structure<sup>24</sup> as well as the cooling curves of pulsars. Contrary to previous estimates<sup>20</sup>, low temperature quark matter is a superconductor of second kind and thus the magnetic field can penetrate into the quark core in Abrikosov vortices and does not decay at timescales shorter than  $10^7$  years. Thus the occurrence of superconducting quark matter phase in compact stars does not contradict observational data<sup>24</sup>. The recently developed nonperturbative approaches to diquark condensates in high-density quark matter<sup>21,22,23</sup> can be further constrained by studying the consequences for cooling curves of pulsars<sup>25</sup> which have to be consistent with the observational data<sup>26</sup>.

## 7 Conclusions

A simple confining separable interaction Ansatz for the rainbow-ladder truncated QCD Dyson-Schwinger equations is found capable of modeling  $\bar{q}q$  meson states at  $T > 0$  together with quark deconfinement and chiral restoration. Deconfinement and chiral restoration are found to both occur at  $T_c = 146$  MeV. The spatial screening masses for the meson modes are obtained. We find that, until near  $T_c$ ,  $M_\pi(T)$  and  $f_\pi(T)$  are weakly  $T$ -dependent and that this model obeys the exact QCD pseudoscalar mass relation to better than 1%. The GMOR relation is found to be accurate to within 5% until very near  $T_c$ . For the vector mode, the 3-space transverse and longitudinal masses  $M_\rho^T(T)$  and  $M_\rho^L(T)$  are weakly  $T$ -dependent while the width for the electromagnetic decay  $\rho^0 \rightarrow e^+e^-$  is found to increase to 1.72 times the  $T = 0$  width. The equation of state (EOS) for the model is investigated in the  $T - \mu$  plane and it shows a tricritical point at  $T = 127$  MeV,  $\mu = 120$  MeV. At  $T = 0$  the EOS can be given the form of a bag model where a broad range of bag constants  $B = 75 \dots 150$  MeV/fm<sup>3</sup> is obtained consistent with possible parametrizations of  $\pi$  and  $\rho$  observables.

The consequences for deconfinement transition in rapidly rotating neutron stars are considered and a new signal from the pulsar timing in binary systems with mass accretion is suggested. The model EOS under consideration meets the new constraints for maximum mass and radius recently derived from QPO observations. Within the present model, quark matter below  $T_c \sim 50$  MeV is a superconductor of second kind and it is suggested that the magnetic field in a neutron star forms an Abrikosov vortex lattice which penetrates into the quark matter core and thus in accordance with the observation does not decay on timescales of  $10^4$  years as previously suggested.

## Acknowledgments

P.C.T. acknowledges support by the NATIONAL SCIENCE FOUNDATION under Grant No. INT-9603385 and the hospitality of the University of Rostock where part of this work was conducted. The work of D.B. has been supported in part by the Deutscher Akademischer Austauschdienst (DAAD) and by the Volkswagen Stiftung under grant No. I/71 226. The authors thank Yu. Kalinovsky, P. Maris, C.D. Roberts and S. Schmidt for discussions and criticism.

## References

1. *Quark Matter '97*, Proceedings of the XI International Conference, Tsukuba, Japan, Nucl. Phys. **A 638** (1998).
2. A. Bender, D. Blaschke, Yu.L. Kalinovsky, C.D. Roberts, Phys. Rev. Lett. **77** (1996) 3724.
3. D. Blaschke, C.D. Roberts, S. Schmidt, Phys. Lett. **B 425** (1998) 232.
4. P. Maris, C.D. Roberts, S. Schmidt, Phys. Rev. **C 57** (1998) R2821.
5. D. Blaschke, C.D. Roberts, Nucl. Phys. **A 642** (1998) 197.
6. P.C. Tandy, Prog. Part. Nucl. Phys. **39** (1997) 117.
7. C.J. Burden, Lu Qian, C.D. Roberts, P.C. Tandy and M.J. Thomson, Phys. Rev. **C 55** (1997) 2649.
8. D. Blaschke, Yu.L. Kalinovsky and P. Tandy, in: Proc. of the XI Int. Conf. on *Problems of Quantum Field Theory*, Dubna, July 13-17, 1998; hep-ph/9811476.
9. H. Munczek and Nemirovsky, Phys. Rev. **D28** (1982) 3081.
10. P. Maris, C.D. Roberts and P.C. Tandy, Phys. Lett. **B420** (1998) 267.
11. M.A. Ivanov, Yu.L. Kalinovsky and C.D. Roberts, nucl-th/9812063, to appear in Phys. Rev. D, 1999.
12. H.-J. Schulze and D. Blaschke, Phys. Lett. **B 386** (1996) 429, and references therein.
13. J.I. Kapusta, *Finite temperature field theory*, Cambridge University Press, Cambridge, 1989.
14. M. Stephanov, K. Rajagopal and E. Shuryak, Phys. Rev. Lett. **81** (1998) 4816; M. Stephanov, these proceedings.
15. D. Blaschke and M. Buballa, in preparation.
16. N.K. Glendenning, *Compact stars*, Springer, New York, 1997.
17. E. Chubarian, H. Grigorian, G. Poghosyan and D. Blaschke, *Deconfinement transition in rotating compact stars*, astro-ph/9903489.
18. F.K. Lamb, M.C. Miller and D. Psaltis, astro-ph/9802089, and references therein.
19. N.K. Glendenning, S. Pei and F. Weber, Phys. Rev. Lett. **79** (1997)

- 1603.
20. D. Bailin and A. Love, Phys. Rep. **107** (1984) 325.
  21. M. Alford, K. Rajagopal and F. Wilczek, Phys. Lett. **B 422** (1998) 247.
  22. R. Rapp, T. Schäfer, E.V. Shuryak and M. Velkovsky, Phys. Rev. Lett. **81** (1998) 53.
  23. G.W. Carter and D. Diakonov, *Light quarks in the Instanton Vacuum at finite Baryon Density* hep-ph/9812445.
  24. D. Blaschke, D.M. Sedrakian and K.M. Shahabasyan, *Diquark condensates and the magnetic field of pulsars*, astro-ph/9904395.
  25. D. Blaschke, T. Klähn, A.D. Sedrakian and D.N. Voskresensky, in preparation.
  26. S. Tsuruta, Comments Ap. **11** (1986) 151.